propagation are directly accessible to anyone with basic statistical knowledge. This should ultimately open the way for a complete characterization of the roles of direct and indirect top-down and bottom-up mechanisms involved in the regulation of parasite densities (fig. S12 and table S1) in the context of both single and mixed infections, and how this in turn affects transmission and disease severity.

The underlying process of bursting infected RBCs and invasion of uninfected RBCs is common to blood-phase malaria across animal taxa. The methods we introduce will consequently be generally applicable. The strength of the mouse data we have used is the finely resolved measures of uninfected and infected red blood cells. We are unaware of any experimental time series in human patients in which these parameters were directly measured, but our analyses suggest that future longitudinal studies of individual patients that undertake the simple assays required to directly assess RBC densities in addition to parasite densities will lead to considerable insights into the factors regulating human malaria.

### References and Notes

1. R. Carter, D. Walliker, *Ann. Trop. Med. Parasitol.* **69**, 187 (1975).
2. L. Molineaux, M. Träuble, W. E. Collins, G. M. Jeffery, K. Dietz, *Trans. R. Soc. Trop. Med. Hyg.* **96**, 205 (2002).
3. K. Dietz, G. Raddatz, L. Molineaux, *Am. J. Trop. Med. Hyg.* **75** (suppl.), 46 (2006).
4. D. T. Haydon, L. Matthews, R. Timms, N. Colegrave, *Proc. R. Soc. B* **270**, 289 (2003).
5. R. M. Ribeiro *et al.*, *J. Virol.* **84**, 6096 (2010).
6. O. N. Bjørnstad, B. Finkenstädt, B. T. Grenfell, *Ecol. Monogr.* **72**, 169 (2002).
7. R. M. Anderson, R. M. May, *Infectious Diseases of Humans* (Oxford Univ. Press, Oxford, 1991).
8. M. A. Nowak, R. M. May, *Virus Dynamics: Mathematical Principles of Immunology and Virology* (Oxford Univ. Press, Oxford, 2000).
9. M. M. Stevenson, E. M. Riley, *Nat. Rev. Immunol.* **4**, 169 (2004).
10. M. Walther *et al.*, *J. Immunol.* **177**, 5736 (2006).
11. M. R. Miller, L. Råberg, A. F. Read, N. J. Savill, *PLOS Comput. Biol.* **6**, e1000946 (2010).
12. N. Mideo *et al.*, *Am. Nat.* **172**, E214 (2008).
13. R. Antia, A. Yates, J. C. de Roode, *Proc. R. Soc. B* **275**, 1449 (2008).
14. B. F. Kochin, A. J. Yates, J. C. de Roode, R. Antia, *PLoS ONE* **5**, e10444 (2010).
15. A. Handel, I. M. Longini Jr., R. Antia, *J. R. Soc. Interface* **7**, 35 (2010).
16. C. L. Ball, M. A. Gilchrist, D. Coombs, *Bull. Math. Biol.* **69**, 2361 (2007).
17. A. S. Perelson, *Nat. Rev. Immunol.* **2**, 28 (2002).
18. R. A. Saenz *et al.*, *J. Virol.* **84**, 3974 (2010).
19. K. A. Lythgoe, L. J. Morrison, A. F. Read, J. D. Barry, *Proc. Natl. Acad. Sci. U.S.A.* **104**, 8095 (2007).
20. L. Molineaux, K. Dietz, *Parassitologia* **41**, 221 (1999).
21. R. Killick-Kendrick, W. Peters, Eds., *Rodent Malaria* (Academic Press, London, 1978).
22. V. C. Barclay *et al.*, *Proc. R. Soc. B* **275**, 1171 (2008).
23. S. Huijben, thesis, University of Edinburgh (2010).
24. G. H. Long, B. H. K. Chan, J. E. Allen, A. F. Read, A. L. Graham, *BMC Evol. Biol.* **8**, 128 (2008).
25. See supporting material on *Science* Online.
26. P. G. McQueen, F. E. McKenzie, *Proc. Natl. Acad. Sci. U.S.A.* **101**, 9161 (2004).
27. B. Hellriegel, *Proc. R. Soc. B* **250**, 249 (1992).
28. C. Hetzel, R. M. Anderson, *Parasitology* **113**, 25 (1996).
29. W. Jarra, K. N. Brown, *Parasitology* **99**, 157 (1989).
30. A. A. Lamikanra *et al.*, *Blood* **110**, 18 (2007).
31. S. S. Pilyugin, R. Antia, *Bull. Math. Biol.* **62**, 869 (2000).
32. R. Antia, J. C. Koella, *J. Theor. Biol.* **168**, 141 (1994).
33. J. R. Glynn, D. J. Bradley, *Parasitology* **110**, 7 (1995).
34. M. S. Russell *et al.*, *J. Immunol.* **179**, 211 (2007).
35. D. L. Chao, M. P. Davenport, S. Forrest, A. S. Perelson, *Immunol. Cell Biol.* **82**, 55 (2004).
36. R. Stephens, J. Langhorne, *PLoS Pathog.* **6**, e1001208 (2010).
37. C. Othoro *et al.*, *J. Infect. Dis.* **179**, 279 (1999).
38. F. P. Mockenhaupt *et al.*, *Blood* **104**, 2003 (2004).
39. S. Wambua, J. Mwacharo, S. Uyoga, A. Macharia, T. N. Williams, *Br. J. Haematol.* **133**, 206 (2006).
40. K. Baer, C. Klotz, S. H. Kappe, T. Schnieder, U. Frevert, *PLoS Pathog.* **3**, e171 (2007).
41. N. J. Savill, W. Chadwick, S. E. Reece, *PLOS Comput. Biol.* **5**, e1000416 (2009).
42. Z. Su, A. Fortin, P. Gros, M. M. Stevenson, *J. Infect. Dis.* **186**, 1321 (2002).
43. G. H. Long, B. H. K. Chan, J. E. Allen, A. F. Read, A. L. Graham, *Parasitology* **133**, 673 (2006).
44. K.-H. Chang, M. Tam, M. M. Stevenson, *J. Infect. Dis.* **189**, 735 (2004).

# A Large and Persistent Carbon Sink in the World's Forests

Yude Pan,[1]* Richard A. Birdsey,[1] Jingyun Fang,[2,3] Richard Houghton,[4] Pekka E. Kauppi,[5] Werner A. Kurz,[6] Oliver L. Phillips,[7] Anatoly Shvidenko,[8] Simon L. Lewis,[7] Josep G. Canadell,[9] Philippe Ciais,[10] Robert B. Jackson,[11] Stephen W. Pacala,[12] A. David McGuire,[13] Shilong Piao,[2] Aapo Rautiainen,[5] Stephen Sitch,[7] Daniel Hayes[14]

The terrestrial carbon sink has been large in recent decades, but its size and location remain uncertain. Using forest inventory data and long-term ecosystem carbon studies, we estimate a total forest sink of $2.4 \pm 0.4$ petagrams of carbon per year (Pg C year$^{-1}$) globally for 1990 to 2007. We also estimate a source of $1.3 \pm 0.7$ Pg C year$^{-1}$ from tropical land-use change, consisting of a gross tropical deforestation emission of $2.9 \pm 0.5$ Pg C year$^{-1}$ partially compensated by a carbon sink in tropical forest regrowth of $1.6 \pm 0.5$ Pg C year$^{-1}$. Together, the fluxes comprise a net global forest sink of $1.1 \pm 0.8$ Pg C year$^{-1}$, with tropical estimates having the largest uncertainties. Our total forest sink estimate is equivalent in magnitude to the terrestrial sink deduced from fossil fuel emissions and land-use change sources minus ocean and atmospheric sinks.

Forests have an important role in the global carbon cycle and are valued globally for the services they provide to society. International negotiations to limit greenhouse gases require an understanding of the current and potential future role of forest C emissions and sequestration in both managed and unmanaged forests. Estimates by the Intergovernmental Panel on Climate Change (IPCC) show that the net uptake by terrestrial ecosystems ranges from less than 1.0 to as much as 2.6 Pg C year$^{-1}$ for the 1990s (*1*). More recent global C analyses have estimated a terrestrial C sink in the range of 2.0 to 3.4 Pg C year$^{-1}$ on the basis of atmospheric CO$_2$ observations and inverse modeling, as well as land observations (*2–4*). Because of this uncertainty and the possible change in magnitude over time, constraining these estimates is critically important to support future climate mitigation actions.

[1]U.S. Department of Agriculture Forest Service, Newtown Square, PA 19073, USA. [2]Key Laboratory for Earth Surface Processes, Ministry of Education, Peking University, Beijing, 100871 China. [3]State Key Laboratory of Vegetation and Environmental Change, Institute of Botany, Chinese Academy of Sciences, Beijing, 100093 China. [4]Woods Hole Research Center, Falmouth, MA 02543, USA. [5]University of Helsinki, Helsinki, Finland. [6]Natural Resources Canada, Canadian Forest Service, Victoria, BC, V8Z 1M5, Canada. [7]School of Geography, University of Leeds, LS2 9JT, UK. [8]International Institute for Applied Systems Analysis, Laxenburg, Austria. [9]Global Carbon Project, Commonwealth Scientific and Industrial Research Organization Marine and Atmospheric Research, Canberra, Australia. [10]Laboratoire des Sciences du Climat et de l'Environnement CEA-UVSQ-CNRS, Gif sur Yvette, France. [11]Duke University, Durham, NC 27708, USA. [12]Princeton University, Princeton, NJ 08544, USA. [13]U.S. Geological Survey, Alaska Cooperative Fish and Wildlife Research Unit, University of Alaska, Fairbanks, AK 99775, USA. [14]Oak Ridge National Laboratory, Oak Ridge, TN 37831, USA.

*To whom correspondence should be addressed. E-mail: ypan@fs.fed.us

Here, we present bottom-up estimates of C stocks and fluxes for the world's forests based on recent inventory data and long-term field observations coupled to statistical or process models (table S1). We advanced our analyses by including comprehensive C pools of the forest sector (dead wood, harvested wood products, living biomass, litter, and soil) and report past trends and changes in C stocks across countries, regions, and continents representing boreal, temperate, and tropical forests (5, 6). To gain full knowledge of the tropical C balance, we subdivided tropical forests into intact and regrowth forests (Table 1). The latter is an overlooked category, and its C uptake is usually not reported but is implicit in the tropical land-use change emission estimates. Although deforestation, reforestation, afforestation and the carbon outcomes of various management practices are included in the assessments of boreal and temperate forest C sink estimates, we separately estimated three major fluxes in the tropics: C uptake by intact forests, losses from deforestation, and C uptake of forest regrowth after anthropogenic disturbances. The area of global forests used as a basis for estimating C stocks and fluxes is 3.9 billion ha, representing 95% of the world's forests (7) (table S2).

**Global forest C stocks and changes.** The current C stock in the world's forests is estimated to be $861 \pm 66$ Pg C, with $383 \pm 30$ Pg C (44%) in soil (to 1-m depth), $363 \pm 28$ Pg C (42%) in live biomass (above and below ground), $73 \pm 6$ Pg C (8%) in deadwood, and $43 \pm 3$ Pg C (5%) in litter

(table S3). Geographically, $471 \pm 93$ Pg C (55%) is stored in tropical forests, $272 \pm 23$ Pg C (32%) in boreal, and $119 \pm 6$ Pg C (14%) in temperate forests. The C stock density in tropical and boreal forests is comparable (242 versus 239 Mg C ha$^{-1}$), whereas the density in temperate forests is ~60% of the other two biomes (155 Mg C ha$^{-1}$). Although tropical and boreal forests store the most carbon, there is a fundamental difference in their carbon structures: Tropical forests have 56% of carbon stored in biomass and 32% in soil, whereas boreal forests have only 20% in biomass and 60% in soil.

The average annual change in the C stock of established forests (Table 1) indicates a large uptake of $2.5 \pm 0.4$ Pg C year$^{-1}$ for 1990 to 1999 and a similar uptake of $2.3 \pm 0.5$ Pg C year$^{-1}$ for 2000 to 2007. Adding the C uptake in tropical regrowth forests to those values indicates a persistent global gross forest C sink of $4.0 \pm 0.7$ Pg C year$^{-1}$ over the two periods (Tables 1 and 2). Despite the consistency of the global C sink since 1990, our analysis revealed important regional and temporal differences in sink sizes. The C sink in temperate forests increased by 17% in 2000 to 2007 compared with 1990 to 1999, in contrast to C uptake in intact tropical forests, which decreased by 23% (but nonsignificantly). Boreal forests, on average, showed little difference between the two time periods (Fig. 1). Subtracting C emission losses from tropical deforestation and degradation, the global net forest C sink was $1.0 \pm 0.8$ and $1.2 \pm 0.9$ Pg C year$^{-1}$ for

1990 to 1999 and 2000 to 2007, respectively (Table 1).

**Forest carbon sinks by regions, biomes, and pools.** Boreal forests (1135 Mha) had a consistent average sink of $0.5 \pm 0.1$ Pg C year$^{-1}$ for two decades (Table 2, 20 and 22% of the global C sinks in established forests). However, the overall stability of the boreal forest C sink is the net result of contrasting carbon dynamics in different boreal countries and regions associated with natural disturbances and forest management. Asian Russia had the largest boreal sink, but that sink showed no overall change, even with increased emissions from wildfire disturbances (8). In contrast, there was a notable sink increase of 35% in European Russia (Fig. 1) attributed to several factors: increased areas of forests after agricultural abandonment, reduced harvesting, and changes of forest age structure to more productive stages, particularly for the deciduous forests (8). In contrast to the large increase of biomass sinks in European Russia and northern Europe (8, 9), the biomass C sink in Canadian managed forests was reduced by half between the two periods, mostly due to the biomass loss from intensified wildfires and insect outbreaks (10, 11). A net loss of soil C in northern Europe was attributed to shifts of forest to nonforest in some areas. Overall, the relatively stable boreal C sink is the sum of a net reduction in Canadian biomass sink offset by increased biomass sink in all other boreal regions, and a balance between decreased litter and soil C sinks in northern Eurasia and a region-wide increase in the accumulation of dead wood (Table 2).

Temperate forests (767 Mha) contributed $0.7 \pm 0.1$ and $0.8 \pm 0.1$ Pg C year$^{-1}$ (27 and 34%) to the global C sinks in established forests for two decades (Table 2). The primary reasons for the increased C sink in temperate forests are the increasing density of biomass and a substantial increase in forest area (12, 13). The U.S. forest C sink increased by 33% from the 1990s to 2000s, caused by increasing forest area; growth of existing immature forests that are still recovering from historical agriculture, grazing, harvesting (12, 14); and environmental factors such as $CO_2$ fertilization and N deposition (15). However, forests in the western United States have shown considerably increased mortality over the past few decades, related to drought stress, and increased mortality from insects and fires (16, 17). The European temperate forest sink was stable between 1990 to 1999 and 2000 to 2007. There was a large C sink in soil due to expansion of forests in the 1990s, but this trend slowed in the 2000s (7, 18). However, the increased C sink in biomass during the second period (+17%) helped to maintain the stability of the total C sink. China's forest C sink increased by 34% between 1990 to 1999 and 2000 to 2007, with the biomass sink almost doubling (Table 2). This was caused primarily by increasing areas of newly planted forests, the consequence of an intensive national afforestation/reforestation program in the past few decades (table S2) (19).

**Table 1.** Global forest carbon budget (Pg C year$^{-1}$) over two time periods. Sinks are positive values; sources are negative values.

| Carbon sink and source in biomes | 1990–1999 | 2000–2007 | 1990–2007 |
|---|---|---|---|
| Boreal forest | $0.50 \pm 0.08$ | $0.50 \pm 0.08$ | $0.50 \pm 0.08$ |
| Temperate forest | $0.67 \pm 0.08$ | $0.78 \pm 0.09$ | $0.72 \pm 0.08$ |
| Tropical intact forest* | $1.33 \pm 0.35$ | $1.02 \pm 0.47$ | $1.19 \pm 0.41$ |
| Total sink in global established forests† | $2.50 \pm 0.36$ | $2.30 \pm 0.49$ | $2.41 \pm 0.42$ |
| Tropical regrowth forest‡ | $1.57 \pm 0.50$ | $1.72 \pm 0.54$ | $1.64 \pm 0.52$ |
| Tropical gross deforestation emission§ | $-3.03 \pm 0.49$ | $-2.82 \pm 0.45$ | $-2.94 \pm 0.47$ |
| Tropical land-use change emission‖ | $-1.46 \pm 0.70$ | $-1.10 \pm 0.70$ | $-1.30 \pm 0.70$ |
| Global gross forest sink¶ | $4.07 \pm 0.62$ | $4.02 \pm 0.73$ | $4.05 \pm 0.67$ |
| Global net forest sink# | $1.04 \pm 0.79$ | $1.20 \pm 0.85$ | $1.11 \pm 0.82$ |

*Equations of global forest C fluxes*

$$F_{\text{established forests}} = F_{\text{boreal forests}} + F_{\text{temperate forests}} + F_{\text{tropical intact forests}} \quad \text{(Eq. 1)}$$
$$F_{\text{tropical land-use change}} = F_{\text{tropical gross deforestation}} + F_{\text{tropical regrowth forests}} \quad \text{(Eq. 2)}$$
$$F_{\text{gross forest sink}} = F_{\text{established forests}} + F_{\text{tropical regrowth forests}} \quad \text{(Eq. 3)}$$
$$F_{\text{net forest sink}} = F_{\text{established forests}} + F_{\text{tropical land-use change}} \quad \text{(Eq. 4)}$$

*Tropical intact forests: tropical forests that have not been substantially affected by direct human activities; flux accounts for the dynamics of natural disturbance-recovery processes. †Global established forests: the forest remaining forest over the study periods plus afforested land in boreal and temperate biomes, in addition to intact forest in the tropics (Eq. 1). ‡Tropical regrowth forests: tropical forests that are recovering from past deforestation and logging. §Tropical gross deforestation: the total C emissions from tropical deforestation and logging, not counting the uptake of C in tropical regrowth forests. ‖Tropical land-use change: emissions from tropical land-use change, which is a net balance of tropical gross deforestation emissions and C uptake in regrowth forests (Eq. 2). It may be referenced as a tropical net deforestation emission in the literature. ¶Global gross forest sink: the sum of total sinks in global established forests and tropical regrowth forests (Eq. 3). #Global net forest sink: the net budget of global forest fluxes (Eq. 4). It can be calculated in two ways: (i) total sink in global established forests minus tropical land-use change emission or (ii) total global gross forest sink minus tropical gross deforestation emission.

**Table 2.** Estimated annual change in C stock (Tg C year$^{-1}$) by biomes by country or region for the time periods of 1990 to 1999 and 2000 to 2007. Estimates include C stock changes on "forest land remaining forest land" and "new forest land" (afforested land). The uncertainty calculation refers to the supporting online material. ND, data not available; [1], litter is included in soils.

| Biome and country/ region | 1990–1999 | | | | | | | | 2000–2007 | | | | | | | |
|---|---|---|---|---|---|---|---|---|---|---|---|---|---|---|---|---|
| | Biomass | Dead wood | Litter | Soil | Harvested wood product | Total stock change | Uncertainty (±) | Stock change per area (Mg C ha$^{-1}$ year$^{-1}$) | Biomass | Dead wood | Litter | Soil | Harvested wood product | Total stock change | Uncertainty (±) | Stock change per area (Mg C ha$^{-1}$ year$^{-1}$) |
| | (Tg C year$^{-1}$) | | | | | | | | (Tg C year$^{-1}$) | | | | | | | |
| | | | | | | *Boreal** | | | | | | | | | | |
| Asian Russia | 61 | 66 | 63 | 45 | 19 | 255 | 64 | 0.39 | 69 | 97 | 43 | 42 | 13 | 264 | 66 | 0.39 |
| European Russia | 37 | 10 | 22 | 36 | 41 | 146 | 37 | 0.93 | 84 | 19 | 35 | 35 | 26 | 199 | 50 | 1.21 |
| Canada | 6 | −24 | 14 | 6 | 23 | 26 | 7 | 0.11 | −53 | 16 | 19 | 7 | 21 | 10 | 3 | 0.04 |
| European boreal† | 13 | 0 | 3 | 38 | 11 | 65 | 16 | 1.12 | 21 | 0 | 4 | −10 | 13 | 27 | 7 | 0.45 |
| Subtotal | 117 | 53 | 103 | 125 | 94 | 493 | 76 | 0.45 | 120 | 132 | 101 | 74 | 73 | 499 | 83 | 0.44 |
| | | | | | | *Temperate** | | | | | | | | | | |
| United States‡ | 118 | 6 | 13 | 9 | 33 | 179 | 34 | 0.72 | 147 | 9 | 18 | 37 | 28 | 239 | 45 | 0.94 |
| Europe | 117 | 2 | 8 | 81 | 24 | 232 | 58 | 1.71 | 137 | 2 | 9 | 65 | 27 | 239 | 60 | 1.68 |
| China | 60 | 22 | 15 | 31 | 7 | 135 | 34 | 0.96 | 115 | 24 | 8 | 28 | 7 | 182 | 45 | 1.22 |
| Japan | 24 | 9 | ND | 19 | 2 | 54 | 14 | 2.28 | 23 | 5 | ND | 8 | 2 | 37 | 9 | 1.59 |
| South Korea | 6 | 2 | ND | 5 | 0 | 14 | 4 | 2.14 | 12 | 2 | ND | 4 | 0 | 18 | 5 | 2.86 |
| Australia | 17 | ND | 10 | 15 | 8 | 50 | 13 | 0.33 | 17 | ND | 10 | 14 | 10 | 51 | 13 | 0.34 |
| New Zealand | 1 | 0 | 0 | 1 | 5 | 7 | 2 | 0.91 | 1 | 0 | 0 | 1 | 6 | 9 | 2 | 1.05 |
| Other countries | 1 | ND | ND | ND | 0 | 1 | 1 | 0.07 | 2 | 0 | 0 | 0 | 0 | 3 | 2 | 0.18 |
| Subtotal | 345 | 42 | 46 | 160 | 80 | 673 | 78 | 0.91 | 454 | 42 | 45 | 156 | 80 | 777 | 89 | 1.03 |
| | | | | | | *Tropical intact* | | | | | | | | | | |
| Asia | 125 | 13 | 2 | ND | 5 | 144 | 38 | 0.88 | 100 | 10 | 2 | ND | 6 | 117 | 30 | 0.90 |
| Africa | 469 | 48 | 7 | ND | 9 | 532 | 302 | 0.94 | 425 | 43 | 6 | ND | 8 | 482 | 274 | 0.94 |
| Americas | 573 | 48 | 9 | ND | 22 | 652 | 166 | 0.77 | 345 | 45 | 5 | ND | 23 | 418 | 386 | 0.53 |
| Subtotal | 1167 | 109 | 17 | ND | 35 | 1328 | 347 | 0.84 | 870 | 98 | 13 | ND | 36 | 1017 | 474 | 0.71 |
| Global subtotal§ | 1630 | 204 | 166 | 286 | 209 | 2494 | 363 | 0.73 | 1444 | 273 | 158 | 230 | 189 | 2294 | 489 | 0.69 |
| | | | | | | *Tropical regrowth* | | | | | | | | | | |
| Asia | 498 | ND | [1] | 27 | ND | 526 | 263 | 3.52 | 564 | ND | [1] | 30 | ND | 593 | 297 | 3.53 |
| Africa | 169 | ND | [1] | 73 | ND | 242 | 121 | 1.48 | 188 | ND | [1] | 83 | ND | 271 | 135 | 1.47 |
| Americas | 694 | ND | [1] | 113 | ND | 807 | 403 | 4.67 | 745 | ND | [1] | 113 | ND | 858 | 429 | 4.56 |
| Subtotal | 1361 | ND | [1] | 213 | ND | 1574 | 496 | 3.24 | 1497 | ND | [1] | 226 | ND | 1723 | 539 | 3.19 |
| | | | | | | *All tropics‖* | | | | | | | | | | |
| Asia | 623 | 13 | 2 | 27 | 5 | 670 | 266 | 2.14 | 664 | 10 | 2 | 30 | 6 | 711 | 298 | 2.38 |
| Africa | 638 | 48 | 7 | 73 | 9 | 774 | 325 | 1.06 | 613 | 43 | 6 | 83 | 8 | 753 | 305 | 1.08 |
| Americas | 1267 | 48 | 9 | 113 | 22 | 1458 | 436 | 1.42 | 1090 | 45 | 5 | 113 | 23 | 1276 | 577 | 1.30 |
| Subtotal | 2529 | 109 | 17 | 213 | 35 | 2903 | 605 | 1.40 | 2367 | 98 | 13 | 226 | 36 | 2740 | 718 | 1.38 |
| Global total¶ | 2991 | 204 | 166 | 498 | 209 | 4068 | 615 | 1.04 | 2941 | 273 | 158 | 456 | 189 | 4017 | 728 | 1.04 |

*Carbon outcomes of forest land-use changes (deforestation, reforestation, afforestation, and management practices) are included in the estimates in boreal and temperate forests.    †Estimates for the area that includes Norway, Sweden, and Finland.    ‡Estimates for the continental U.S. and a small area in southeast Alaska.    §Estimates for global established forests.    ‖Estimates for all tropical forests including tropical intact and regrowth forests.    ¶Areas excluded from this table include interior Alaska (51 Mha in 2007), northern Canada (118 Mha in 2007), and "other wooded land" reported to the Food and Agriculture Organization.

Tropical intact forests (1392 Mha) represent ~70% of the total tropical forest area (1949 Mha) that accounts for the largest area of global forest biomes (~50%). We used two networks of permanent monitoring sites spanning intact tropical forest across Africa (*20*) and South America (*21*) and assumed that forest C stocks of Southeast Asia (9% of total intact tropical forest area) are changing at the mean rate of Africa and South America, as we lack sufficient data in Southeast Asia to make robust estimates. These networks are large enough to capture the disturbance-recovery dynamics of intact forests (*6*, *20*, *22*). We estimate a sink of 1.3 ± 0.3 and 1.0 ± 0.5 Pg C year$^{-1}$ for 1990 to 1999 and 2000 to 2007,
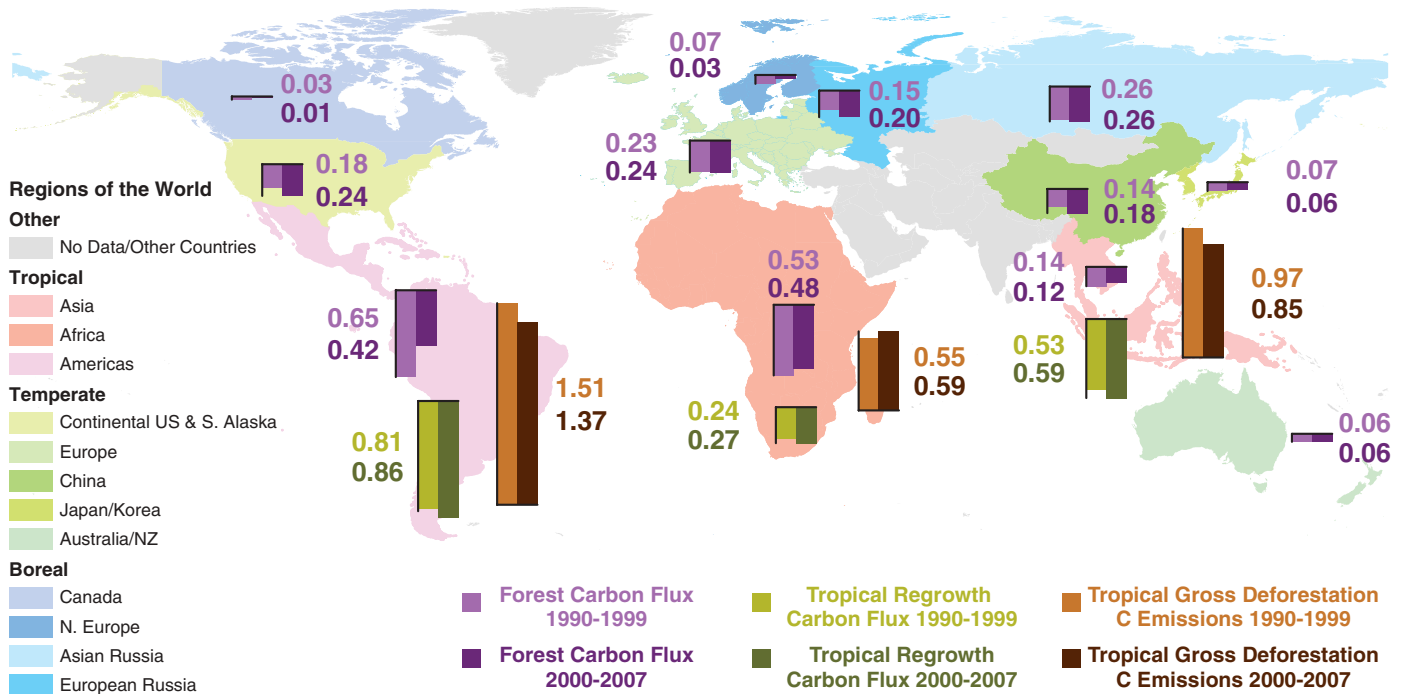
**Fig. 1.** Carbon sinks and sources (Pg C year$^{-1}$) in the world's forests. Colored bars in the down-facing direction represent C sinks, whereas bars in the upward-facing direction represent C sources. Light and dark purple, global established forests (boreal, temperate, and intact tropical forests); light and dark green, tropical regrowth forests after anthropogenic disturbances; and light and dark brown, tropical gross deforestation emissions.

respectively (Table 2). An average C sink of 1.2 ± 0.4 Pg C year$^{-1}$ for 1990 to 2007 is approximately half of the total global C sink in established forests (2.4 ± 0.4 Pg C year$^{-1}$) (Table 1). When only the biomass sink is considered, about two-thirds of the global biomass C sink in established forests is from tropical intact forests (1.0 versus 1.5 Pg C year$^{-1}$). The sink reduction in the period 2000 to 2007 (–23%) was caused by deforestation reducing intact forest area (–8%) and a severe Amazon drought in 2005 (21), which appeared strong enough to affect the tropics-wide decadal C sink estimate (–15%). Except for the Amazon drought, the recent excess of biomass C gain (growth) over loss (death) in tropical intact forests appears to result from progressively enhanced productivity (20, 21, 23). Increased dead biomass production should lead to enhanced soil C sequestration, but we lack data about changes in soil C stocks for tropical intact forests, so the C sink for tropical intact forests may be underestimated.

Tropical land-use changes have caused net C releases in tropical regions by clearing forests for agriculture, pasture, and timber (24), second in magnitude to fossil fuel emissions (Table 3). Tropical land-use change emissions are a net balance of C fluxes consisting of gross tropical deforestation emissions partially compensated by C sinks in tropical forest regrowth. They declined from 1.5 ± 0.7 Pg C year$^{-1}$ in the 1990s to 1.1 ± 0.7 Pg C year$^{-1}$ for 2000 to 2007 (Table 1) due to reduced rates of deforestation and increased forest regrowth (25). The tropical land-use change emissions were approximately equal to the total

**Table 3.** The global carbon budget for two time periods (Pg C year$^{-1}$). There are different arrangements to account for elements of the global C budget (see also table S6). Here, the accounting was based on global C sources and sinks. The terrestrial sink was the residual derived from constraints of two major anthropogenic sources and the sinks in the atmosphere and oceans. We used the C sink in global established forests as a proxy for the terrestrial sink.

| Sources and sinks | 1990–1999 | 2000–2007 |
|---|---|---|
| *Sources (C emissions)* | | |
| Fossil fuel and cement* | 6.5 ± 0.4 | 7.6 ± 0.4 |
| Land-use change† | 1.5 ± 0.7 | 1.1 ± 0.7 |
| Total sources | 8.0 ± 0.8 | 8.7 ± 0.8 |
| *Sinks (C uptake)* | | |
| Atmosphere† | 3.2 ± 0.1 | 4.1 ± 0.1 |
| Ocean‡ | 2.2 ± 0.4 | 2.3 ± 0.4 |
| Terrestrial (established forests)§ | 2.5 ± 0.4 | 2.3 ± 0.5 |
| Total sinks | 7.9 ± 0.6 | 8.7 ± 0.7 |
| Global residuals‖ | 0.1 ± 1.0 | 0.0 ± 1.0 |

*See (2). †See (4, 7, 25). The global land-use change emission is approximately equal to the tropical land-use change emission, because the net carbon balance of land-use changes in temperate and boreal regions is neutral (24, 38). ‡See (4). §Estimates of C sinks in the global established forests (that are outside the areas of tropical land-use changes) from this study. Note that the carbon sink in tropical regrowth forests is excluded because it is included in the term of land-use change emission (see above and Table 1). ‖Global C residuals are close to zero when averaged over a decade. Uncertainties in the global residuals indicate either a land sink or source in the 212 Mha of forest not included here, on nonforest land, or systematic error in other source (overestimate) or sink (underestimate) terms, or both.

global land-use emissions (Tables 1 and 3), because effects of land-use changes on C were roughly balanced in extratropics (7, 24, 25).

Tropical deforestation produced significant gross C emissions of 3.0 ± 0.5 and 2.8 ± 0.5 Pg C year$^{-1}$, respectively, for 1990 to 1999 and 2000 to 2007, ~40% of the global fossil fuel emissions. However, these large emission numbers are usually neglected because more than one half was

offset by large C uptake in tropical regrowth forests recovering from the deforestation, logging, or abandoned agriculture.

Tropical regrowth forests (557 Mha) represent ~30% of the total tropical forest area. The C uptake by tropical regrowth forests is usually implicitly included in estimated net emissions of tropical land-use changes rather than estimated independently as a sink (24). We estimate that

the C sink by tropical regrowth forests was 1.6 ± 0.5 and 1.7 ± 0.5 Pg C year$^{-1}$, respectively, for 1990 to 1999 and 2000 to 2007. Our results indicate that tropical regrowth forests were stronger C sinks than the intact forests due to rapid biomass accumulation under succession, but these estimates are poorly constrained because of sparse data (table S4) (6). Although distinguishing a C sink in tropical regrowth forests does not affect the estimated net emissions from tropical land-use changes, an explicit estimate of this component facilitates evaluating the complete C sink capacity of all tropical and global forests.

When all tropical forests, both intact and regrowth, are combined, the tropical sinks sum to 2.9 ± 0.6 and 2.7 ± 0.7 Pg C year$^{-1}$ over the two periods (Table 1), and on average account for ~70% of the gross C sink in the world forests (~4.0 Pg C year$^{-1}$). However, with equally significant gross emissions from tropical deforestation (Table 1), tropical forests were nearly carbon-neutral. In sum, the tropics have the world's largest forest area, the most intense contemporary land-use change, and the highest C uptake, but also the greatest uncertainty, showing that investment in better understanding carbon cycling in the tropics should be a high priority in the future.

Deadwood, litter, soil, and harvested wood products together accounted for 35% of the global sink and 60% of the global forest C stock, showing the importance of including these components (Table 2 and table S3). Compared with biomass, estimates of these terrestrial carbon pools are generally less certain because of insufficient data. For deadwood, there was a large sink increase in boreal forests over the past decade, caused by the recent increase in natural disturbances in Siberia and Canada. Increased deadwood carbon thus makes a major (27%) but possibly transient contribution to the total C sink in the boreal zone. Changes in litter C accounted for a relatively small and stable portion of the global forest C sink. However, litter C accumulation contributed 20% of the total C sink in boreal forests and, like deadwood, is vulnerable to wildfire disturbances. Changes in soil C stocks accounted for more than 10% of the total sink in the world's forests, largely driven by land-use changes. We may underestimate global soil C stocks and fluxes because the standard 1-m soil depth excludes some deep organic soils in boreal and tropical peat forests (26–28). We estimate the net C change in harvested wood products (HWP), including wood in use and disposed in landfills, as described in the IPCC guidelines (29), attributing changes in stock to the region where the wood was harvested. Carbon sequestration in HWP accounted for ~8% of the total sink in established forests. This sink remained stable for temperate and tropical regions but declined dramatically in boreal regions because of reduced harvest in Russia in the past decade.

**Data gaps, uncertainty, and suggested improvements in global forest monitoring.** We estimated uncertainties based on a combination of quantitative methods and expert opinions (6).

There are critical data gaps that affected both the results presented here and our ability to report and verify changes in forest C stocks in the future. Data are substantially lacking for areas of the boreal forest in North America, including Alaska (51 Mha) and Canadian unmanaged forests (118 Mha) (table S5). The forests in these regions could be a small C source or sink, based on the estimate of Canadian managed forests (10) and modeling studies in Alaska (30). There is also a lack of measurement data of soil C flux in tropical intact forests, which may cause uncertainty of 10 to 20% of the estimated total C sink in these forest areas. In addition, there is a large uncertainty associated with the estimate of C stocks and fluxes in tropical Asia, due to the absence of long-term field measurements, and a notable lack of data about regrowth rates of tropical forests worldwide.

Prioritized recommendations for improvements in regional forest inventories to assess C density, uptake, and emissions for global-scale aggregation include the following: (i) Land monitoring should be greatly expanded in the tropics and in unsampled regions of northern boreal forests. (ii) Globally consistent remote sensing of land-cover change and forest-area is required to combine the strengths of two observation systems: solid ground truth of forest C densities from inventories and reliable forest areas from remote sensing. (iii) Improved methods and greater sampling intensity are needed to estimate non-living C pools, including soil, litter, and dead wood. (iv) Better data are required in most regions for estimating lateral C transfers in harvested wood products and rivers.

**Forest carbon in the global context.** The new C sink estimates from world's forests can contribute to the much needed detection and attribution that is required in the context of the global carbon budget (2, 4, 25). Our results suggest that, within the limits of reported uncertainty, the entire terrestrial C sink is accounted for by C uptake of global established forests (Table 3), as the balanced global budget yields near-zero residuals with ±1.0 Pg C year$^{-1}$ uncertainty for both 1990 to 1999 and 2000 to 2007 (Table 3). Consequently, our results imply that nonforest ecosystems are collectively neither a major (>1 Pg) C sink nor a major source over the two time periods that we monitored. Because the tropical gross deforestation emission is mostly compensated by the C uptakes in both tropical intact and regrowth forests (Fig. 1 and Table 1), the net global forest C sink (1.1 ± 0.8 Pg C year$^{-1}$) resides mainly in the temperate and boreal forests, consistent with previous estimates (31, 32). Notably, the total gross C uptake by the world's established and tropical regrowth forests is 4.0 Pg C year$^{-1}$, which is equivalent to half of the fossil fuel C emissions in 2009 (4). Over the period that we studied (1990 to 2007), the cumulative C sink into the world's established forests was ~43 Pg C and 73 Pg C for the established plus regrowing forests; the latter equivalent to 60% of cumulative fossil emissions in the period (i.e., 126 Pg C).

Clearly, forests play a critical role in the Earth's terrestrial C sinks and exert strong control on the evolution of atmospheric $CO_2$.

**Drivers and outlook of forest carbon sink.** The mechanisms affecting the current C sink in global forests are diverse, and their dynamics will determine its future longevity. The C balance of boreal forests is driven by changes in harvest patterns, regrowth over abandoned farmlands, and increasing disturbance regimes. The C balance of temperate forests is primarily driven by forest management, through low harvest rates (Europe) (33), recovery from past harvesting and agricultural abandonment (U.S.) (34), and large-scale afforestation (China) (19). For tropical forests, deforestation and forest degradation are dominant causes of C emissions, with regrowth and an increase in biomass in intact forests being the main sinks balancing the emissions (23, 24).

Changes in climate and atmospheric drivers ($CO_2$, N-deposition, ozone, diffuse light) affect the C balance of forests, but it is difficult to separate their impacts from other factors using ground observations. For Europe, the U.S., China, and the tropics, evidence from biogeochemical process models suggests that climate change, increasing atmospheric $CO_2$, and N deposition are, at different levels, important factors driving the long-term C sink (15, 18, 20, 23, 34). Drought in all regions and warmer winters in boreal regions reduce the forest sink through suppressed gross primary production, increased tree mortality, increased fires, and increased insect damage (8, 10, 18, 21, 30, 35, 36).

Our estimates suggest that currently the global established forests, which are outside the areas of tropical land-use changes, alone can account for the terrestrial C sink (~2.4 Pg C year$^{-1}$). The tropics are the dominant terms in the exchange of $CO_2$ between the land and the atmosphere. A large amount of atmospheric $CO_2$ has been sequestrated by the natural system of forested lands (~4.0 Pg C year$^{-1}$), but the benefit is substantially offset by the C losses from tropical deforestation (~2.9 Pg C year$^{-1}$). This result highlights the potential for the United Nations Reducing Emissions from Deforestation and Degradation program to lessen the risk of climate change. However, an important caveat is that adding geological carbon from fossil fuels into the contemporary carbon cycle and then relying on biospheric sequestration is not without risk, because such sequestration is reversible from either climate changes, direct human actions, or a combination of both.

Nonetheless, C sinks in almost all forests across the world (Fig. 1) may suggest overall favorable conditions for increasing stocks in forests and wood products. Our analysis also suggests that there are extensive areas of relatively young forests with potential to continue sequestering C in the future in the absence of accelerated natural disturbance, climate variability, and land-use change. As a result of the large C stocks in both boreal forest soils and tropical forest biomass, warming in the boreal zone, deforestation,

and occasional extreme drought, coincident with fires in the tropics, represent the greatest risks to the continued large C sink in the world's forests (21, 24, 30, 37). A better understanding of the role of forests in biosphere C fluxes and mechanisms responsible for forest C changes is critical for projecting future atmospheric $CO_2$ growth and guiding the design and implementation of mitigation policies.

### Reference and Notes

1. G. J. Nabuurs *et al.*, in *Climate Change 2007: Mitigation*, B. Metz, O. R. Davidson, P. R. Bosch, R. Dave, L. A. Meyer, Eds. (Cambridge Univ. Press, Cambridge, 2007), pp. 542–584.
2. J. G. Canadell *et al.*, *Proc. Natl. Acad. Sci. U.S.A.* **104**, 18866 (2007).
3. S. Khatiwala, F. Primeau, T. Hall, *Nature* **462**, 346 (2009).
4. C. Le Quéré *et al.*, *Nat. Geosci.* **2**, 831 (2009).
5. R. K. Dixon *et al.*, *Science* **263**, 185 (1994).
6. Details of data sources, accounting, and estimation methods used for each country, region, and C component are provided in the supporting online material.
7. Food and Agriculture Organization, *Global Forest Resources Assessment 2010* (Food and Agriculture Organization, Rome, 2010), forestry paper 163.
8. A. Z. Shvidenko, D. G. Schepaschenko, S. Nilsson, in *Basic Problems of Transition to Sustainable Forest Management in Russia*, V. A. Sokolov, A. Z. Shvidenko, O. P. Vtorina, Eds. (Russian Academy of Sciences, Krasnoyarsk, Russia, 2007), pp. 5–35.
9. P. E. Kauppi *et al.*, *For. Ecol. Manage.* **259**, 1239 (2010).
10. W. A. Kurz, G. Stinson, G. J. Rampley, C. C. Dymond, E. T. Neilson, *Proc. Natl. Acad. Sci. U.S.A.* **105**, 1551 (2008).
11. G. Stinson *et al.*, *Glob. Change Biol.* **17**, 2227 (2011).
12. R. Birdsey, K. Pregitzer, A. Lucier, *J. Environ. Qual.* **35**, 1461 (2006).
13. P. E. Kauppi *et al.*, *Proc. Natl. Acad. Sci. U.S.A.* **103**, 17574 (2006).
14. Y. Pan *et al.*, *Biogeosciences* **8**, 715 (2011).
15. Y. Pan, R. Birdsey, J. Hom, K. McCullough, *For. Ecol. Manage.* **259**, 151 (2009).
16. P. J. van Mantgem *et al.*, *Science* **323**, 521 (2009).
17. D. D. Breshears *et al.*, *Proc. Natl. Acad. Sci. U.S.A.* **102**, 15144 (2005).
18. P. Ciais *et al.*, *Nat. Geosci.* **1**, 425 (2008).
19. J. Fang, A. Chen, C. Peng, S. Zhao, L. Ci, *Science* **292**, 2320 (2001).
20. S. L. Lewis *et al.*, *Nature* **457**, 1003 (2009).
21. O. L. Phillips *et al.*, *Science* **323**, 1344 (2009).
22. M. Gloor *et al.*, *Glob. Change Biol.* **15**, 2418 (2009).
23. S. L. Lewis, J. Lloyd, S. Sitch, E. T. A. Mitchard, W. F. Laurance, *Annu. Rev. Ecol. Syst.* **40**, 529 (2009).
24. R. A. Houghton, *Annu. Rev. Earth Planet. Sci.* **35**, 313 (2007).
25. P. Friedlingstein *et al.*, *Nat. Geosci.* **3**, 811 (2010).
26. C. Tarnocai *et al.*, *Global Biogeochem. Cycles* **23**, GB2023 (2009).
27. A. Hooijer *et al.*, *Biogeosciences* **7**, 1505 (2010).
28. S. E. Page, J. O. Rieley, C. J. Banks, *Glob. Change Biol.* **17**, 798 (2011).
29. Intergovernmental Panel on Climate Change, *IPCC Guidelines for National Greenhouse Gas Inventories* (Institute for Global Environmental Strategies, Japan, 2006); www.ipcc-nggip.iges.or.jp/public/2006gl/index.html.
30. A. D. McGuire *et al.*, *Ecol. Monogr.* **79**, 523 (2009).
31. C. L. Goodale *et al.*, *Ecol. Appl.* **12**, 891 (2002).
32. J. L. Sarmiento *et al.*, *Biogeosciences* **7**, 2351 (2010).
33. E. D. Schulze *et al.*, *Nat. Geosci.* **2**, 842 (2009).
34. S. W. Pacala *et al.*, *Science* **292**, 2316 (2001).
35. O. L. Phillips *et al.*, *Philos. Trans. R. Soc. London Ser. B* **359**, 381 (2004).
36. J. M. Metsaranta, W. A. Kurz, E. T. Neilson, G. Stinson, *Tellus* **62B**, 719 (2010).
37. M. Zhao, S. W. Running, *Science* **329**, 940 (2010).
38. R. A. Houghton, *Tellus* **55B**, 378 (2003).

# REPORTS

# Detection of Emerging Sunspot Regions in the Solar Interior

Stathis Ilonidis,* Junwei Zhao, Alexander Kosovichev

Sunspots are regions where strong magnetic fields emerge from the solar interior and where major eruptive events occur. These energetic events can cause power outages, interrupt telecommunication and navigation services, and pose hazards to astronauts. We detected subsurface signatures of emerging sunspot regions before they appeared on the solar disc. Strong acoustic travel-time anomalies of an order of 12 to 16 seconds were detected as deep as 65,000 kilometers. These anomalies were associated with magnetic structures that emerged with an average speed of 0.3 to 0.6 kilometer per second and caused high peaks in the photospheric magnetic flux rate 1 to 2 days after the detection of the anomalies. Thus, synoptic imaging of subsurface magnetic activity may allow anticipation of large sunspot regions before they become visible, improving space weather forecast.

Understanding solar magnetism is among the most important problems of solar physics and astrophysics (1–5). Modern theories assume that sunspot regions are generated by a dynamo action at the bottom of the convection zone, about 200 Mm below the photosphere. However, there is no convincing observational evidence to support this idea, and dynamo mechanisms operating in the bulk of the convection zone or even in the near-surface shear layer have been proposed as well (6, 7). Investigation of emerging magnetic flux could possibly determine the depth of this process and set the foundations for a better understanding of sunspots and active regions.

Active regions on the Sun produce flares and mass eruptions that may cause power outages on Earth, satellite failures, and interruptions of telecommunication and navigation services. Monitoring solar subsurface processes and predicting magnetic activity would also improve space weather forecasts.

Time-distance helioseismology (8) is one of the local helioseismology techniques that image acoustic perturbations in the interior of the Sun (9). Acoustic waves are excited by turbulent convection near the surface, propagate deep inside the Sun, and are refracted back to the surface (Fig. 1). Time-distance helioseismology measures travel times of acoustic waves propagating to different distances by computing cross-covariances between the oscillation signals observed at pairs of locations on the solar photosphere. Variations in acoustic travel times are caused mainly by thermal perturbations, magnetic fields, and flows. Previous studies of emerging sunspot regions (10–14) have found difficulties in detecting signals deeper than 30 Mm and before the initial magnetic field becomes visible on the surface because of the fast emergence speed and low signal-to-noise ratio (15). Here, we present a deep-focus time-distance measurement scheme, which allows us to detect signals of emerging magnetic regions in the deep solar interior (16, 17).

We have used Doppler observations (18) from Michelson Doppler Imager (MDI) (19) onboard the Solar and Heliospheric Observatory (SOHO) and computed travel-time maps of four emerging flux regions and nine quiet regions. In Fig. 2, we present the results of our analysis for Active Region (AR) 10488, which started emerging on the solar disc at 09:30 UT, 26 October 2003, about

W. W. Hansen Experimental Physics Laboratory, Stanford University, Stanford, CA 94305–4085, USA

*To whom correspondence should be addressed. E-mail: ilonidis@sun.stanford.edu